



UNIVERSITY OF LEEDS

This is a repository copy of *Automated modelling of spatially-distributed glacier ice thickness and volume*.

White Rose Research Online URL for this paper:
<http://eprints.whiterose.ac.uk/99553/>

Version: Accepted Version

Article:

James, WHM and Carrivick, J (2016) Automated modelling of spatially-distributed glacier ice thickness and volume. *Computers & Geosciences*, 92. pp. 90-103. ISSN 0098-3004

<https://doi.org/10.1016/j.cageo.2016.04.007>

© 2016, Elsevier. Licensed under the Creative Commons Attribution-NonCommercial-NoDerivatives 4.0 International
<http://creativecommons.org/licenses/by-nc-nd/4.0/>

Reuse

Unless indicated otherwise, fulltext items are protected by copyright with all rights reserved. The copyright exception in section 29 of the Copyright, Designs and Patents Act 1988 allows the making of a single copy solely for the purpose of non-commercial research or private study within the limits of fair dealing. The publisher or other rights-holder may allow further reproduction and re-use of this version - refer to the White Rose Research Online record for this item. Where records identify the publisher as the copyright holder, users can verify any specific terms of use on the publisher's website.

Takedown

If you consider content in White Rose Research Online to be in breach of UK law, please notify us by emailing eprints@whiterose.ac.uk including the URL of the record and the reason for the withdrawal request.



eprints@whiterose.ac.uk
<https://eprints.whiterose.ac.uk/>

Automated modelling of spatially-distributed glacier ice thickness and volume

William H.M. James*¹ and Jonathan L. Carrivick¹

¹School of Geography, University of Leeds, Woodhouse Lane, Leeds, West Yorkshire, LS2 9JT, UK.

*correspondence to:

William James,

Email: gy06whmj@leeds.ac.uk

Tel.: 0113 34 33345

Abstract

Ice thickness distribution and volume are both key parameters for glaciological and hydrological applications. This study presents VOLTA (Volume and Topography Automation), which is a Python script tool for ArcGIS™ that requires just a digital elevation model (DEM) and glacier outline(s) to model distributed ice thickness, volume and bed topography. Ice thickness is initially estimated at points along an automatically generated centreline network based on the perfect-plasticity rheology assumption, taking into account a valley side drag component of the force balance equation. Distributed ice thickness is subsequently interpolated using a glaciologically correct algorithm. For five glaciers with independent field-measured bed topography, VOLTA modelled volumes were between 26.5 % (underestimate) and 16.6 % (overestimate) of that derived from field observations. Greatest differences were where an asymmetric valley cross section shape was present or where significant valley infill had occurred. Compared with other methods of modelling ice thickness and volume, key advantages of VOLTA are: a fully automated approach and a user friendly graphical user interface (GUI), GIS consistent geometry, fully automated centreline generation, inclusion of a side drag component in the force balance equation, estimation of glacier basal shear stress for each individual glacier, fully distributed ice thickness output and the ability to process multiple glaciers rapidly. VOLTA is capable of regional scale ice volume assessment, which is a key parameter for exploring glacier response to climate change. VOLTA also permits subtraction of modelled ice thickness from the input surface elevation to produce an ice-free DEM, which is a key input for reconstruction of former glaciers. VOLTA could assist with prediction of future glacier geometry changes and hence in projection of future meltwater fluxes.

Keywords: ice thickness distribution, glacier volume, subglacial topography, glacier centrelines, perfect-plasticity

40 **1 Introduction**

41

42 Knowledge of contemporary regional ice thickness distribution is poor (Farinotti et al. 2009), with field
43 measurements impractical and data requirements making larger scale modelling studies difficult. In
44 the context of ongoing climate change, large scale assessments are important because a climate signal
45 extracted from an individual glacier may not be representative of the entire region (Hoelzle et al.
46 2007). Furthermore, it is total regional ice volume that is essential for exploring the response of
47 glaciers to climate change (Chinn et al. 2012) and for the projection of meltwater availability (Kaser et
48 al. 2010). Ice thickness distribution is required for glacier dynamics models (e.g. Oerlemans et al. 1998)
49 and for assessing the impact of climate change on the hydrology of glaciated catchments (e.g. Huss et
50 al. 2008). Glacier bed topography derived via distributed ice thickness estimations can be used to
51 reconstruct palaeoglaciers (Benn and Hulton 2010), and the resultant equilibrium-line altitudes are a
52 widely-used source of palaeoclimatic information (e.g. Benn and Ballantyne 2005). Glacier bed
53 topography is also of great assistance in understanding glaciological hazards, such as jökulhlaups
54 routing from or sourced subglacially (e.g. Carrivick 2007; Staines and Carrivick 2015), and for
55 understanding subglacial lake formation (Frey et al. 2010). Therefore, the development of methods
56 for assessing regional ice thickness distribution is essential for improving our understanding of many
57 glaciological, hydrological and climatological issues.

58

59 Distributed ice thickness and ice volume can either be calculated by interpolating field measurements
60 or by modelling. Ice thickness can be measured via boreholes (e.g. Hochstein et al. 1998) or by
61 reflection techniques such as seismics (e.g. Shean et al. 2007) or radar (e.g. Singh et al. 2012). Although
62 impractical for regional scale studies, field measurements are crucial to parameterise (e.g. Bahr et al.
63 1997) and validate (e.g. Li et al. 2012) models. Due to the logistical and technical difficulties of field
64 measurement, scaling laws are often employed to estimate glacier volumes at regional scales (Bahr et
65 al. 1997). However, scaling approaches do not account for individual glacier characteristics and do not
66 yield information on bed topography. Furthermore, errors may be in excess of 50 % for individual
67 glaciers, reducing to 25 % for regional volume (Meier et al. 2007).

68

69 A variety models to estimate ice thickness based on viscous flow mechanics and mass turnover are
70 available (e.g. Farinotti et al. 2009; McNabb et al. 2012; Michel et al. 2013), and they have ability to
71 estimate ice thickness with an accuracy of ~25 % (Farinotti et al. 2009). However, these existing models
72 invariably require glacier specific datasets such as mass balance (e.g. Michel et al. 2013), surface
73 velocity fields (e.g. McNabb et al. 2012) or the manual digitization of flowlines and ice flow catchments

74 (Farinotti et al. 2009), limiting their use for regional scale application. A neural network approach has
75 also been developed (Clarke et al. 2009), although it has only been tested against artificial “horizontal
76 lake-like” glaciers and is acknowledged to be computationally intensive, limiting its effectiveness for
77 regional studies.

78

79 An alternative approach utilises the perfect plasticity assumption (Nye 1951), that glacier ice thickness
80 (h) can be found from a glacier surface slope α by the relation:

81

$$82 \quad h = \frac{\tau_b}{f p g \tan \alpha} \quad (1)$$

83

84 Where p is ice density (typically 900 kg m^{-3}), g is gravitational acceleration (9.81 m s^{-2}), τ_b is basal
85 shear stress and f a ‘shape factor’ to incorporate the effect of side drag. With high resolution digital
86 elevation models (DEMs) permitting accurate calculation of surface slope, perfect plasticity based
87 models are proving popular, requiring just glacier outline(s), centreline(s) and a DEM. The relative
88 simplicity of the calculations, combined with wide availability of input datasets are key advantages
89 over viscous flow mechanics models when considering large regions. Whilst basic perfect plasticity
90 models have been used to estimate 3D bed topography (e.g. Linsbauer et al. 2009), more complex
91 models which account for variations in side drag have only been applied in 2D (e.g. Li et al. 2012).
92 Furthermore, all the models to date require manual digitisation of centrelines, limiting their
93 applicability to large regional scale studies.

94

95 The aim of this paper is to present VOLTA (Volume and Topography Automation), which is a tool for
96 rapid estimation of distributed ice thickness. Key advantages of VOLTA are: a fully automated
97 approach and a user friendly graphical user interface (GUI), GIS consistent geometry, automatic
98 centreline generation, inclusion of a side drag component in the force balance equation, individual
99 glacier basal shear stress estimation, fully distributed ice thickness and bed topography outputs, and
100 the ability to process multiple glaciers rapidly

101

102 **1.1 Volume and Topography Automation (VOLTA)**

103

104 VOLTA estimates ice thickness along automatically derived centrelines and interpolates fully
105 distributed ice thickness. It can be applied on multiple glaciers of complex geometry, requiring just
106 glacier outline(s) and a DEM as inputs. VOLTA is written in the Python scripting language and executed
107 via ArcGIS™ as a geoprocessing tool. VOLTA, installation instructions and manual are available for

108 download at: <https://github.com/williamjames/volta>. A schematic flowchart of the VOLTA workflow
109 is presented in Figure 1.

110 **2 Theory**

111 **2.1 Automating centreline production**

112
113 VOLTA initially estimates ice thickness along automatically derived centrelines. Whilst it would be
114 desirable to derive centrelines which represent actual flowlines (i.e. ice trajectories), this would
115 require fully distributed velocity fields, making regional scale applications unachievable (Kienholz et
116 al. 2014). Whilst centrelines will usually coincide with the location of maximum ice thickness along a
117 traverse profile, they may be offset in some circumstances, such as in the vicinity of sharp bends.

118
119 Traditionally, centreline production required manual digitization, a time consuming and subjective
120 process. Recently, automated techniques using GIS hydrology tools (Schiefer et al. 2008; Machguth
121 and Huss 2014), cost-distance analysis (Kienholz et al. 2014) and geometric analysis (Le Bris and Paul
122 2013) have been developed, although only appearing in the literature with regards to method
123 development. To overcome the constraints of manually digitizing centrelines, VOLTA generates
124 centreline(s) using the glacier axis concept (Le Bris and Paul 2013). VOLTA develops the algorithm by:

125

- 126 • Improving the axis creation technique
- 127 • Automatically adjusting the smoothing parameter.
- 128 • Automatically creating separate centrelines for multiple tributaries.
- 129 • Incorporating the algorithm with VOLTA

130

131 Firstly, a glacier axis is created to define the main direction of the glacier. Whereas Le Bris and Paul
132 (2013) determined the axis by joining the highest and lowest points of the glacier, VOLTA uses a
133 minimum bounding geometry (MBG) technique, followed by connecting the two farthest points (Fig.
134 2a). This creates an axis not influenced by individual high and low DEM cells, which may otherwise
135 create an unrealistic axis. Perpendicular traverses are created along the axis at the resolution of the
136 DEM, which are subsequently clipped to the glacier outline and midpoints placed on each traverse
137 segment (Fig. 2b).

138

139 An initial centreline is constructed by iteratively joining traverse midpoints (starting at the highest
140 midpoint) in a similar manner to that described by (Le Bris and Paul 2013). The line is then smoothed
141 using the Polynomial Approximation with Exponential Kernel (PAEK) algorithm to remove irregularities

142 caused by small scale variations in glacier shape. Larger glaciers require greater smoothing as wide
 143 tributaries result in a smooth course of the centreline (Kienholz et al. 2014). The amount of smoothing
 144 is controlled by glacier area in an approach similar to that of Kienholz et al. (2014):

145

$$146 \quad l = \begin{cases} 2 \cdot 10^{-6} \cdot A + 200 & : l \leq l_{max} \\ l_{max} & : l > l_{max} \end{cases} \quad (2)$$

147

148 Where l is smoothing length, A is glacier area (m^2) and l_{max} is 1,000 m

149

150 **2.2. Glaciers of complex geometry**

151

152 A single centreline may not be suitable if the glacier is of complex geometry due to multiple tributaries
 153 or cirques (Fig. 2e). Whilst the lack of a secondary tributary centreline is the main issue, the initial
 154 centreline is also laterally deflected where the perpendicular traverses are elongated as they continue
 155 into the secondary tributary (Fig. 2d). To overcome these issues, VOLTA uses a novel ‘upstream area’
 156 approach to delineate separate tributaries, allowing multiple centrelines to be generated (Fig. 2e).
 157 Iteratively working down the initial centreline, upstream area is calculated. Total area will steadily
 158 increase down-centreline, but a marked increase occurs when a new tributary enters (Fig. 3). VOLTA
 159 calculates area at an interval equal to 1 % of centreline length with a new tributary identified if area
 160 increases by > 30 % between successive points. Furthermore, any new tributary must also have an
 161 area of at least 20 % of the total. Whilst these thresholds may be altered via the GUI, testing against
 162 manually identified tributaries for 25 glaciers found these values were able to correctly delineate
 163 tributaries where appropriate, whilst not adding ‘extra’ tributaries due to small areas of ice adjoining.
 164 If secondary tributaries are identified, new tributary outlines are created from a subset of the original
 165 (Fig. 2e) and secondary centrelines are created in the standard manner, ignoring any midpoints of
 166 which the corresponding perpendicular crosses into another tributary. Branch order is managed in the
 167 same manner as Kienholz et al. (2014), with the initial centreline classed as the primary centreline.

168

169 **2.3 Calculating ice thickness at points along the centreline**

170

171 VOLTA estimates thickness along the centreline(s) using a perfect plasticity approach (Eq. 1). For
 172 mountain valley glaciers, a shape factor (f) is required because valley sides support part of the weight
 173 of the glacier, resulting in τ_b on the centreline being lower than for an infinitely wide basin. f can be
 174 incorporated as a constant (usually 0.8: Nye 1965), a form which has been used extensively in the
 175 literature (e.g. Linsbauer et al. 2012).

176

177 Li et al. (2012) developed a more physically realistic method which dynamically adjusts f depending
 178 on the local width of the glacier (see Li et al. (2012) for a full-derivation):

179

$$180 \quad h = \frac{0.9 w \left(\frac{\tau_b}{pg \sin \alpha} \right)}{0.9 w - \left(\frac{\tau_b}{pg \sin \alpha} \right)} \quad (3)$$

181

182 Where w is half the glacier width at the specified point.

183

184 Whilst Eq. (3) estimates ice thickness perpendicular to the ice surface (Fig. 4a), VOLTA estimates
 185 ‘vertical’ ice thickness, perpendicular to a horizontal x-axis (Fig. 4b), a form appropriate for GIS
 186 geometry:

$$187 \quad h = \frac{0.9 w \left(\frac{\tau_b}{pg \tan \alpha} \right)}{0.9 w - \left(\frac{\tau_b}{pg \tan \alpha} \right)} \quad (4)$$

188

189 For some glacier geometries (e.g. where nunataks are present or where tributaries converge), width
 190 calculation may be inaccurate, with Li et al. (2012) cautioning against its use without cross-checking.
 191 VOLTA automatically checks for erroneous values by: (i) checking if the perpendicular line intersects
 192 another centreline (Fig. 5a) and (ii) cross checking if the resulting f value (Eq. 1) is realistic (> 0.445 ,
 193 equal to a half width to centreline thickness ratio of 1: Nye 1965, Fig. 5b). At points where either of
 194 these conditions are met, VOLTA calculates thickness using Eq. (1), with f set to that of the average for
 195 the tributary (calculated from points on the same tributary with accurate width calculations). The
 196 “f_type” field in the output point file indicates which method is used, with “W” denoting the
 197 independent width has been used and “A” denoting the tributary average value has been used.

198

199 **2.4 Interpolating distributed ice thickness and bed topography**

200

201 VOLTA interpolates distributed ice thickness using the ANUDEM 5.3 interpolation routine, which is an
 202 iterative finite difference technique designed for the creation of hydrologically correct DEMs
 203 (Hutchinson 1989). ANUDEM is implemented via the ‘TopoToRaster’ tool in ArcGIS, using ice thickness
 204 points as ‘spot height’ inputs and the glacier outline(s) as a contour input (assumed to represent zero
 205 ice thickness), with any ice divides ignored. ANUDEM generates preferably concave shaped landforms,
 206 mimicking the typical parabolic shape of (idealised) glacier beds (Linsbauer et al. 2009) and is the
 207 method of choice for interpolating both mountain valley glaciers (Fischer and Kuhn 2013) and ice

208 sheets, such as the Bedmap2 Antarctica dataset (Fretwell et al. 2013). Interpolating of this manner is
 209 an accepted method for bed topography estimation (Farinotti et al. 2009; Li et al. 2012; Linsbauer et
 210 al. 2012), although sediment infill or the compound incision effects of multiple glaciation phases may
 211 result in modified cross sections under some circumstances (Schrott et al. 2003). VOLTA outputs the
 212 raw centreline ice thickness points, allowing bespoke interpolation by the user if required.

213

214 Once thickness h for each cell has been interpolated, total volume, V can be calculated:

215

$$216 \quad V = \sum(c^2h) \quad (5)$$

217 Where c is the cellsize.

218

219 **2.5 VOLTA parameters**

220

221 By default, VOLTA does not require any user specified parameters, using the DEM and glacier
 222 outline(s) to derive glacier specific values. These may be altered if required (e.g. if independent ice-
 223 thickness measurements exist). VOLTA parameters are: basal shear stress (τ_b), slope averaging
 224 distance (α_d), “effective width” slope threshold (α_{lim}) and minimum slope threshold(α_0).

225

226 **2.5.1 Basal shear stress (τ_b)**

227

228 τ_b is variable between individual glaciers due to many factors (e.g. basal water pressure, ice viscosity,
 229 subglacial sediment deformation), meaning no universal value should be used between glaciers. For
 230 modelling, τ_b does not have to be varied longitudinally for an individual glacier as a constant value
 231 can reproduce accurate thickness estimates along the length of a centreline (Li et al. 2012).

232

233 Whilst τ_b can be “constrained reasonably from just a few ice-thickness measurements” (Li et al. 2012
 234 p.7), in the majority of cases there are no independent measurements, requiring τ_b to be estimated.

235 An empirical relationship between altitudinal extent and τ_b developed by Haeberli and Hoelzle (1995)
 236 is often used, although the spread of data points is large ($r^2 = 0.44$), with Linsbauer et al. (2012)
 237 estimating an uncertainty of up to $\pm 45\%$. A more robust relationship was developed by Driedger and
 238 Kennard (1986a), using area and slope in an elevation band approach:

239

$$240 \quad \tau_b = 2.7 \cdot 10^4 \sum_{i=1}^n \left(\frac{A_i}{\cos \alpha_i} \right)^{0.106} \quad (6)$$

241

242 Where the elevation band area (A_i) is in m^2 and shear stress (τ_b) is in Pa. This method was tested by
 243 Driedger and Kennard (1986b) as part of a volume estimation study, finding a standard deviation of
 244 error of 5 % when comparing with measured volumes. This is the default method used by VOLTA, with
 245 A_i and $\cos \alpha_i$ calculated over 200 m elevation bands. The result is a glacier specific average τ_b value
 246 which is consequently applied to each centreline point. Optionally, τ_b may be user defined via the
 247 GUI.

248

249 **2.5.2 Slope averaging distance (α_d)**

250

251 Analysing the centreline gradient over an appropriate distance (α_d) is required for producing reliable
 252 thickness estimates. If α_d is too low, small scale variations in the surface topography will be
 253 reproduced in the bed profile. Conversely, if α_d is too large, variations in the surface topography may
 254 be smoothed or omitted. α_d should be “several times” the local ice thickness (Paterson 1994). The
 255 value is initially set to 10 times the average glacier thickness (\bar{h}), with \bar{h} derived from a volume area
 256 scaling approach (Radić and Hock 2010):

$$257 \quad \bar{h} = \frac{0.2055A^{1.375}}{A} \quad (7)$$

258 Where A is the glacier area and \bar{h} is average ice thickness.

259

260 **2.5.3 Minimum slope threshold (α_0)**

261

262 Using Eq. 4, ice thickness will tend to infinity as surface slope tends to zero, meaning thickness may
 263 be overestimated in flat regions (Li et al. 2012; Farinotti et al. 2009), To overcome this, a ‘minimum
 264 slope threshold’ (α_0) is used in the same manner as Farinotti et al. (2009) and Li et al. (2012), setting
 265 any lower slope values to it. The threshold was determined empirically at 5° by Farinotti et al. (2009)
 266 and 4° by (Li et al. 2012). In VOLTA, α_0 is initially set to 4° , although this may be altered via the GUI if
 267 required.

268

269 **2.5.4 “Effective width” slope threshold (α_{lim})**

270

271 VOLTA accounts for valley side drag by incorporating glacier width (Eq. 4). However, thin ice on higher
 272 parts of the valley wall will contribute negligible support and thus should not be included in the width
 273 calculation. An “effective width” slope threshold (α_{lim}) is used to help exclude those areas as

274 described by Li et al. (2012). In VOLTA, α_{lim} is set by default to 30° , which is the optimal value found
275 during analysis by Li et al. (2012), although this value may be altered via the GUI if required. Using a
276 slope angle of 30° and shear stress values parameterised for the European Alps (130 kPa) and the
277 New Zealand Alps (180 kPa) (Hoelzle et al. 2007), the original perfect plasticity assumption (Eq. 1),
278 estimates ice thickness values of 27 m and 37 m respectively. These thickness values are consistent
279 with Driedger and Kennard (1986a) who found a threshold of average glacier thickness at ~ 36 m
280 where glaciers obtain a critical shear stress and contributed to deformation.

281

282 **3 Results**

283

284 **3.1 Application to glaciers with different geometry**

285

286 For comparison, VOLTA was applied to 5 separate glaciers. Glaciers were selected for: (i) ice thickness
287 distribution that has been well constrained from field measurements; (ii) comprising a range of
288 different spatial scales and geometries (single, multi-tributary); and (iii) occupying different regional
289 settings and thus different thermal and dynamic characteristics. Datasets used to produce the 'field
290 based' ice distributions are summarized in Table 1.

291

292 The Ödenwinkelkees glacier, Austrian Alps (Fig. 6a) is the smallest glacier (1.9 km^2) and is of a relatively
293 simple geometry. South Cascade glacier (Fig. 6b) was chosen due to its exceptionally well constrained
294 bed topography, providing an example of a simple glacier geometry in North America. Storglaciären
295 (Sweden) is more complex, characterised by a branched accumulation area (Fig. 6c), whilst
296 Unteraargletscher (Swiss Alps) provides an example of a larger multi-tributary glacier (Fig. 6e). The
297 Tasman glacier, (New Zealand) and its tributaries form the largest and most complex system, covering
298 90 km^2 (Fig. 6d).

299

300 **3.2 Generating a field based ice thickness distribution dataset**

301

302 Glacier outlines and field observations of ice thickness were digitized, georeferenced and projected in
303 a Cartesian co-ordinate system. To account for ice surface topography changes between thickness
304 measurement and DEM capture (surface lowering, retreat etc.), ice thickness was standardised to the
305 surface DEM by subtracting the bed elevation from the surface DEM. The following analysis is
306 therefore correct for the time of DEM capture. Ice thickness was interpolated using the ANUDEM
307 algorithm (Hutchinson 1989). Due to interpolation and also original error in the ice thickness

308 measurements, the interpolated bed cannot be regarded as a truly accurate representation of the
309 subglacial topography. Whilst the datasets used have no error analysis available, it is assumed to be \pm
310 10 m to account for errors in the raw data collection (Pellikka and Rees 2009) and in digitization. For
311 the Tasman, error is estimated to be \pm 20 m due to the small scale of diagrams from which
312 measurements were digitized (e.g. Hart 2014).

313

314 **3.3 Centreline generation**

315

316 VOLTA generated a single centerline for the Ödenwinkelkees and South cascade glaciers and multiple
317 centerlines for Storglaciären, Unteraargletscher and the Tasman (Fig. 7). Due to the complex nature
318 of the Tasman system and the format of the outline, additional ice divides were digitized between
319 nunataks and the main outline to ensure that individual branches were defined correctly. A
320 combination of DEM inspection and a GIS generated ridgeline network (Fig. 8) was used to inform the
321 location of potential ice divides.

322

323 **3.4 Distributed ice thickness and volume**

324

325 Distributed ice thickness was estimated as described in Fig. 1, with results shown in Fig. 9 and Table 2.
326 Overall volume was estimated to between 26.5 % (underestimate) and 16.6 % (overestimate) of that
327 derived from field measurements (Table 2). Histograms in Fig. 9 graphically display the distribution of
328 deviation between VOLTA and field measurements, with a positive skew (Fig. 9a, 9l) representing an
329 overestimate by VOLTA (Ödenwinkelkees and Unteraargletscher) and a negative skew (Fig. 9f, 9i, 9o)
330 representing an underestimate (South Cascade, Storglaciären, Tasman).

331

332 For Unteraargletscher, both the field measured (Fig. 9a) and modelled (Fig. 9b) ice thickness show a
333 parabolic cross section with the maximum ice thickness situated close to the centreline (Fig. 10a).
334 South Cascade glacier field data reveals an asymmetrical bed cross section (Fig. 9d and 10c), which is
335 not particularly well defined by VOLTA (Fig. 9e and 10c), resulting in a relatively large difference
336 between volume estimated from field data and by VOLTA (Table 2). The parabolic bed profile of
337 Storglaciären shown by field measurements (Fig. 9g and 10e) are well reproduced by VOLTA, with
338 longitudinal variations also defined (Fig. 9h). The good agreement between field data and VOLTA is
339 shown by similar final volume calculations (Table 2). This is also the case of the Ödenwinkelkees, where
340 an overdeepening evident in the field measurements (Fig. 9j) is also predicted by VOLTA (Fig. 9k). For
341 the Tasman system, field measurements on the main branch suggest a bed cross section with a

342 relatively flat base (Fig. 10b), whilst VOLTA predicts a parabolic shape. Despite this, VOLTA is still able
 343 to accurately predict maximum ice thickness on the centerline (Fig. 9n) and total volume (Table 2).

344

345 **3.5 Regional scale modelling: New Zealand Southern Alps**

346

347 The minimal input data requirements and automated approach makes VOLTA ideal for regional scale
 348 modelling. VOLTA was applied to the New Zealand Southern Alps, with Fig. 11 showing an extract for
 349 the Mt. Cook region. VOLTA was applied to 158 glaciers, from which 196 centrelines were produced.
 350 The volume of the Mt. Cook region was calculated to be 19.82 km³ (17.82 km³ water equivalent).
 351 Analysis was performed on a PC with a 3.0 GHz Intel Core i5 processor and 8GB of RAM, with centreline
 352 generation taking an average of 18.4 seconds per glacier and ice thickness distribution taking an
 353 average of 22.1 seconds per glacier.

354

355 **4 Discussion**

356

357 **4.1 Sensitivity testing**

358

359 To ascertain to what extent uncertainties in VOLTA parameters influence volume estimates, sensitivity
 360 tests were performed (Fig. 12). Parameters τ_b , α_d , α_0 and α_{lim} were tested independantly by altering
 361 their value whilst keeping others constant. Parameters were varied within bounds that could be
 362 reasonably expected, with the baseline set to that used for initial volume estimation. For each
 363 parameter, a range of 12 values was used, so Fig. 12 reports a total of 240 model runs.

364

365 τ_b is the most sensitive parameter, showing a similar positive linear relationship for all glaciers (Fig.
 366 12a). For example, a 10% increase in τ_b results in a 12.2% increase in volume for the Ödenwinkelkees.
 367 This is expected as the critical thickness at which deformation occurs will be greater as τ_b is increased
 368 (Paterson 1994). Volume is also sensitive to α_d , with smaller glaciers (Ödenwinkelkees, South Cascade,
 369 Storglaciären) showing a negative relationship (Fig. 12b). An increase in α_d results in fewer thickness
 370 estimation points as no values can be determined at each end of the centreline (to a distance equal
 371 to half of α_d). Interpolations therefore trend to zero sooner, a possible cause of the negative
 372 relationship observed for smaller glaciers. Sensitivity to α_0 is variable (Fig. 12c), with glaciers
 373 dominated by large regions of low gradient ice (e.g. Unteraargletscher) showing a negative
 374 relationship whilst steep glaciers (e.g. Ödenwinkelkees) are not sensitive to α_0 . Likewise the sensitivity
 375 of VOLTA-derived volumes to α_{lim} is variable depending on glacier surface topography; glaciers with

376 large steep accumulation zones (e.g. Tasman) are most sensitive. Overall, it is the volume of small
377 glaciers with areas of extreme gradient (either high or low) that are likely to be most sensitive to
378 VOLTA input parameters. In contrast, the modelled volume of larger glaciers comprising moderate
379 gradient surfaces will be least sensitive to VOLTA input parameters. These factors influencing the
380 sensitivity of VOLTA should inform the choice of glaciers and regions to apply the model to, and should
381 be taken into account when interpreting results.

382

383 **4.2 Centreline generation and glacier length**

384

385 Fig. 7 demonstrates that VOLTA is able to produce centrelines for glaciers of different geometries and
386 size. The main advantages compared to manual centreline production come with the reproducible
387 and fast computation. VOLTA successfully created multiple centrelines where appropriate, although
388 in the most complex system (Tasman) the initial model run revealed that centrelines were not created
389 in some of the tributary branches. To rectify this, adjustment of the outline was performed, with
390 additional ice divides added (Fig. 8). This is a quick process and is likely to affect only a very small
391 proportion of glaciers. Application to the Southern Alps of New Zealand resulted in 18 of the 196 (i.e.
392 9 %) of the centrelines (and one outline polygon) requiring manual adjustment, which is comparable
393 to the original centreline algorithm developed by Le Bris and Paul (2013), which reported adjustment
394 in 13 % of cases.

395

396 **4.3 Total volume estimation**

397

398 VOLTA returned the overall volume to between 26.5 % (underestimate) and 16.6 % (overestimate) of
399 that derived from field measurements (Table 2). For comparison, approximate errors for scaling
400 approaches range from 30 % for large samples to 40 % when considering smaller samples (~ 200
401 glaciers) (Farinotti and Huss 2013). The model presented by Farinotti et al. (2009) had an accuracy of
402 ~25 % inferred from point-to-point comparison of measured and modelled thickness values whilst Li
403 et al. (2012) reproduced measured thicknesses (radar transects) with a mean absolute error of 11.8
404 %. Considering the uncertainty in the field based glacier volume estimates used for benchmarking,
405 VOLTA can be seen to perform at a similar level to other approaches. However, the fully automated
406 and user friendly approach offers advantages over previous models, offering the potential to rapidly
407 model regions which would otherwise be prohibitively laborious. VOLTA is capable of regional scale
408 ice volume assessment (Fig. 11), which is a key parameter for exploring glacier response to climate

409 change, and which has previously been estimated using less sophisticated techniques such as volume-
410 area scaling (e.g. Chinn et al. 2012).

411

412 **4.4 Distributed ice thickness**

413

414 VOLTA results show a visually and statistically good correspondence with those from field
415 measurements. The spatial variations in thickness largely match those shown by the field
416 measurements, with features such as overdeepenings being defined. Modelling of the Mt Cook area
417 (Fig. 11) shows VOLTA is suitable for regional scale modelling on a standard desktop computer.
418 Although no performance metrics are available for alternative methods, overall processing times by
419 VOLTA are expected to be vastly superior due to the minimal input data and complete automation of
420 the process.

421

422 Comparison of modelled and measured ice thickness distributions (Fig. 9) shows that estimating ice
423 thickness along a centreline followed by interpolation using the ANUDEM routine is an acceptable
424 method for determining distributed ice thickness. Where the glacier cross section is a typical parabolic
425 shape (Harbor and Wheeler 1992), VOLTA estimates closely match the field data along the entirety of
426 the cross section (e.g. Fig. 10a, 10e). The Tasman glacier is an example of a contemporary glacier with
427 an infilled bed, resulting in the near-horizontal bed profile visible in the field measurements (Fig. 10b).
428 VOLTA is able to predict the maximum thickness well (VOLTA modelled 496 m versus measured 510
429 m) because the perfect plasticity assumption accounts for the corresponding low bed gradient along
430 the centreline. However, the parabolic profile generated by ANUDEM underestimates ice thickness
431 towards the valley sides, contributing to the 16.4 % overall volume deficit for the Tasman glacier.

432

433 Whilst the centreline will usually approximate the line of maximum thickness, in some cases this may
434 be offset due to bends in the glacier (e.g. Ödenwinkelkees, South Cascade). Whilst VOLTA can still
435 accurately estimate the maximum thickness under such circumstances (Fig. 10c, 10d), this may be
436 offset from the centre, resulting in skewed bed topography (Fig. 10d). This may be overcome by using
437 actual flowlines (i.e. ice trajectories), rather than centrelines, although there is currently no feasible
438 method to generate such inputs on a regional scale.

439

440 In general, VOLTA is able to predict maximum ice thickness values well, even if infilling or multiple past
441 glaciations have occurred. Whilst the ANUDEM interpolation routine generally works well for linear
442 glaciers with a bedrock base (parabolic profile), the user should be aware of potential issues when

443 considering in-filled valleys or glaciers with sharp bends in their centreline. VOLTA outputs the original
444 point ice thickness estimations if the user wishes to use an alternative interpolation routine.

445

446 **4.5 Bed topography and 'ice-free' DEMs**

447

448 Calculation of distributed ice thickness, bed topography and ice volume are all of importance for many
449 glaciological and hydrological applications, whilst the ability of VOLTA to be run on many glaciers in a
450 region simultaneously will be of use in investigations of spatial variability in glacier responses to
451 climate (Carrivick and Chase 2011). Furthermore, VOLTA has the ability to produce an 'ice-free' (bed
452 topography) surface by subtracting the ice thickness from each DEM cell, an essential input for
453 estimating palaeoglacier volume (e.g. Gолledge et al. 2012; Carrivick et al. 2015). VOLTA provides a
454 robust approach for estimating bed topography and therefore has the potential to reduce uncertainty
455 in palaeo ice volume estimates. 'Ice free' surfaces are also useful as a direct input for palaeoglacier
456 reconstruction models (e.g. Benn and Hulton 2010; Schilling and Hollin 1981) and for hazard
457 assessment (Frey et al. 2010). Palaeoglacier reconstructions driven by the 'ice free' DEM generated by
458 VOLTA may be further used for the estimation of former equilibrium line altitudes (ELA), providing
459 one of the few methods for estimating palaeo-precipitation (e.g. Benn and Ballantyne 2005). VOLTA
460 can be seen as a pre-cursor for such studies, potentially improving the accuracy of palaeoclimatic
461 models.

462

463 **5 Conclusions**

464

465 VOLTA is a script tool for the rapid and data-efficient 3D modelling of glaciers: specifically of
466 distributed ice thickness, volume and bed topography. VOLTA requires just a DEM and glacier
467 outline(s) as inputs, both of which can be obtained free of charge with an almost global coverage for
468 research purposes (e.g. GLIMS 2014; USGS 2014). Whilst the basic perfect plasticity assumption is
469 applicable for ice sheets (Nye 1951), VOLTA is optimised for centreline based modelling where glaciers
470 are constrained by topography. As such, VOLTA can be applied with confidence to any alpine style
471 glaciated region where the appropriate datasets are available. Compared with other existing
472 methods, key advantages of VOLTA are: a fully automated workflow, improved centreline generation
473 that can accommodate glaciers with multiple branches, inclusion of a side drag component in the force
474 balance equation, GIS consistent geometry, individual glacier basal shear stress estimation, fully
475 distributed ice thickness and bed topography outputs and a user friendly graphical user interface
476 (GUI). In comparison of VOLTA-derived ice thickness and volume against independent data from five

477 glaciers where the bed topography was well constrained, total volume estimates fell between 26.5 %
 478 (underestimate) and 16.6 % (overestimate) of the volume estimated from field measurements. The
 479 greatest field based-modelled differences were where bed elevation formed an asymmetric valley
 480 shape or valley infilling had occurred.

481

482 With present knowledge of ice thickness distribution being remarkably limited, VOLTA has the
 483 potential to improve our database of estimated ice thickness and thus also of estimated glacier
 484 volume. With the ability to produce an 'ice-free' DEM, an important prerequisite for addressing a
 485 range of glaciological and hydrological issues can be provided quickly.

486

487 **Acknowledgements**

488 Research was supported by a NERC PhD studentship (grant number NE/K500847/1). Peter Jansson is
 489 thanked for the GIS format data for Storglaciären. Ödenwinkelkees ALS data was obtained by JLC and
 490 a team via a European Facility for Airborne Research (EUFAR) Transnational Access award. Duncan
 491 Quincey and Neil Glasser are thanked for their constructive comments and criticism of the paper.
 492 Stefan Winkler and Trevor Chinn are thanked for their insights into New Zealand glaciology.

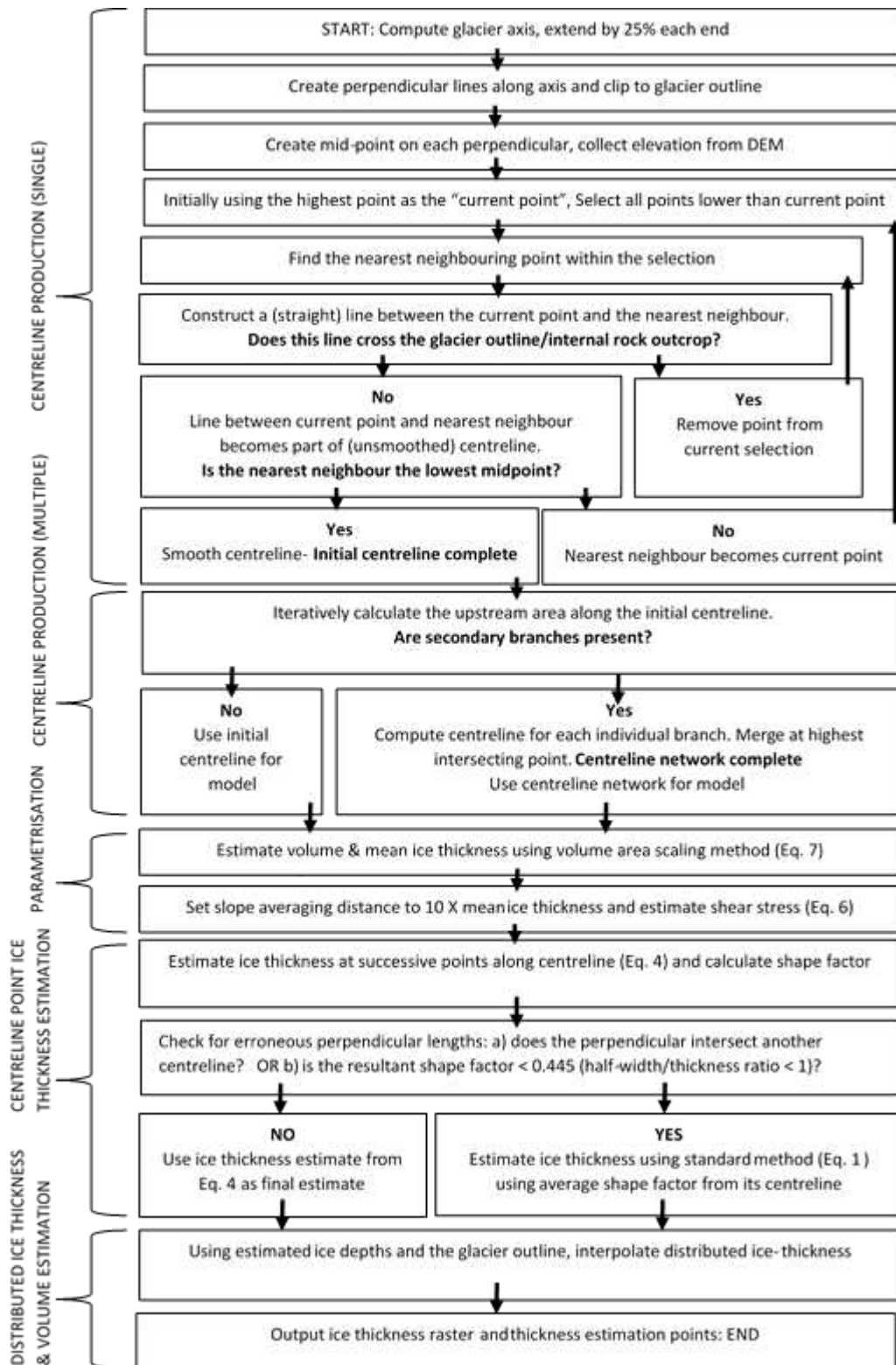
493

494 **References**

- 495 Bahr, D. B., M. F. Meier and S. D. Peckham. 1997. The physical basis of glacier volume-area scaling.
 496 *Journal of Geophysical Research-Solid Earth*, **102**(B9), pp.20355-20362.
- 497 Bauder, A., M. Funk and G. H. Gudmundsson. 2003. The ice-thickness distribution of
 498 Unteraargletscher, Switzerland. *Annals of Glaciology*, **37**(1), pp.331-336.
- 499 Benn, D. I. and C. K. Ballantyne. 2005. Palaeoclimatic reconstruction from Loch Lomond Readvance
 500 glaciers in the West Drumochter Hills, Scotland. *Journal of Quaternary Science*, **20**(6), pp.577-
 501 592.
- 502 Benn, D. I. and N. R. J. Hulton. 2010. An Excel (TM) spreadsheet program for reconstructing the surface
 503 profile of former mountain glaciers and ice caps. *Computers & Geosciences*, **36**(5), pp.605-610.
- 504 Björnsson, H. 1981. Radio-echo sounding maps of Storglaciären, Isfallsglaciären and Rabots Glaciär,
 505 northern Sweden. *Geografiska Annaler. Series A. Physical Geography*, **63**(3), pp.225-231.
- 506 Broadbent, M. 1974. *Seismic and gravity surveys on the Tasman Glacier: 1971-2*. Geophysics Division
 507 Department of Scientific and Industrial Research.
- 508 Carrivick, J. L. 2007. Modelling coupled hydraulics and sediment transport of a high-magnitude flood
 509 and associated landscape change. *Annals of Glaciology*, **45**(1), pp.143-154.
- 510 Carrivick, J. L. et al. 2015. Decadal Scale Changes Of The Ödenwinkelkees, Central Austria, Suggest
 511 Increasing Control of Topography and Evolution Towards Steady State. *Geografiska Annaler:
 512 Series A, Physical Geography*.
- 513 Carrivick, J. L. and S. E. Chase. 2011. Spatial and temporal variability in the net mass balance of glaciers
 514 in the Southern Alps, New Zealand. *New Zealand Journal of Geography and Geophysics*, **54**(4),
 515 pp.415-429.
- 516 Carrivick, J. L. et al. 2013. Contemporary geomorphological activity throughout the proglacial area of
 517 an alpine catchment. *Geomorphology*, **188**, pp.83-95.

- 518 Chinn, T. et al. 2012. Annual ice volume changes 1976–2008 for the New Zealand Southern Alps. *Global*
519 *and Planetary Change*, **92–93**, pp.105-118.
- 520 Clarke, G. K. et al. 2009. Neural networks applied to estimating subglacial topography and glacier
521 volume. *Journal of Climate*, **22**(8), pp.2146-2160.
- 522 Driedger, C. and P. Kennard. 1986a. Glacier volume estimation on Cascade volcanoes: an analysis and
523 comparison with other methods. *Annals of Glaciology*, **8**, pp.59-64.
- 524 Driedger, C. L. and P. M. Kennard. 1986b. *Ice volumes on Cascade volcanoes: Mount Rainier, Mount*
525 *Hood, Three Sisters, and Mount Shasta*. Washington: U.S. Geological Survey Professional
526 Paper 1365
- 527 Farinotti, D. and M. Huss. 2013. An upper-bound estimate for the accuracy of glacier volume–area
528 scaling. *The Cryosphere*, **7**(6), pp.1707-1720.
- 529 Farinotti, D. et al. 2009. A method to estimate the ice volume and ice-thickness distribution of alpine
530 glaciers. *Journal of Glaciology*, **55**(191), pp.422-430.
- 531 Fischer, A. and M. Kuhn. 2013. Ground-penetrating radar measurements of 64 Austrian glaciers
532 between 1995 and 2010. *Annals of Glaciology*, **54**(64), pp.179-188.
- 533 Fountain, A. G. and I. R. W. Jacobel. 1997. Advances in ice radar studies of a temperate alpine glacier,
534 South Cascade Glacier, Washington, VSA. *Annals of Glaciology*, **24**, pp.303 - 308.
- 535 Fretwell, P. et al. 2013. Bedmap2: improved ice bed, surface and thickness datasets for Antarctica. *The*
536 *Cryosphere*, **7**(1).
- 537 Frey, H. et al. 2010. A multi-level strategy for anticipating future glacier lake formation and associated
538 hazard potentials. *Natural Hazards and Earth System Science*, **10**(2), pp.339-352.
- 539 GLIMS. 2014. *GLIMS, and National Snow and Ice Data Center. 2005, updated 2012. GLIMS Glacier*
540 *Database*. Boulder, Colorado USA.
- 541 Gollidge, N. R. et al. 2012. Last Glacial Maximum climate in New Zealand inferred from a modelled
542 Southern Alps icefield. *Quaternary Science Reviews*, **46**, pp.30-45.
- 543 Haeberli, W. and M. Hoelzle. 1995. Application of inventory data for estimating characteristics of and
544 regional climate-change effects on mountain glaciers: A pilot study with the European Alps.
545 *Annals of Glaciology*, **21**, pp.206-212.
- 546 Harbor, J. M. and D. A. Wheeler. 1992. On the mathematical description of glaciated valley cross
547 sections. *Earth Surface Processes and Landforms*, **17**(5), pp.477-485.
- 548 Hart, R. 2014. *The ice thickness distribution of a debris-covered glacier: Tasman Glacier, New Zealand.*
549 thesis, Victoria University of Wellington.
- 550 Hochstein, M. P. et al. 1998. Rapid melting of the terminal section of the Hooker Glacier (Mt Cook
551 National Park, New Zealand). *New Zealand Journal of Geology and Geophysics*, **41**(3), pp.203-
552 218.
- 553 Hoelzle, M. et al. 2007. The application of glacier inventory data for estimating past climate change
554 effects on mountain glaciers: A comparison between the European Alps and the Southern Alps
555 of New Zealand. *Global and Planetary Change*, **56**(1), pp.69-82.
- 556 Huss, M. et al. 2008. Modelling runoff from highly glacierized alpine drainage basins in a changing
557 climate. *Hydrological Processes*, **22**(19), pp.3888-3902.
- 558 Hutchinson, M. 1989. A new procedure for gridding elevation and stream line data with automatic
559 removal of spurious pits. *Journal of Hydrology*, **106**(3), pp.211-232.
- 560 Kaser, G., M. Großhauser and B. Marzeion. 2010. Contribution potential of glaciers to water availability
561 in different climate regimes. *Proceedings of the National Academy of Sciences*, **107**(47),
562 pp.20223-20227.
- 563 Kienholz, C. et al. 2014. A new method for deriving glacier centerlines applied to glaciers in Alaska and
564 northwest Canada. *The Cryosphere*, **8**(2), pp.503-519.
- 565 Le Bris, R. and F. Paul. 2013. An automatic method to create flow lines for determination of glacier
566 length: A pilot study with Alaskan glaciers. *Computers & Geosciences*, **53**, pp.234 - 245.
- 567 Li, H. et al. 2012. An extended "perfect-plasticity" method for estimating ice thickness along the flow
568 line of mountain glaciers. *Journal of Geophysical Research-Earth Surface*, **117**(F01020).

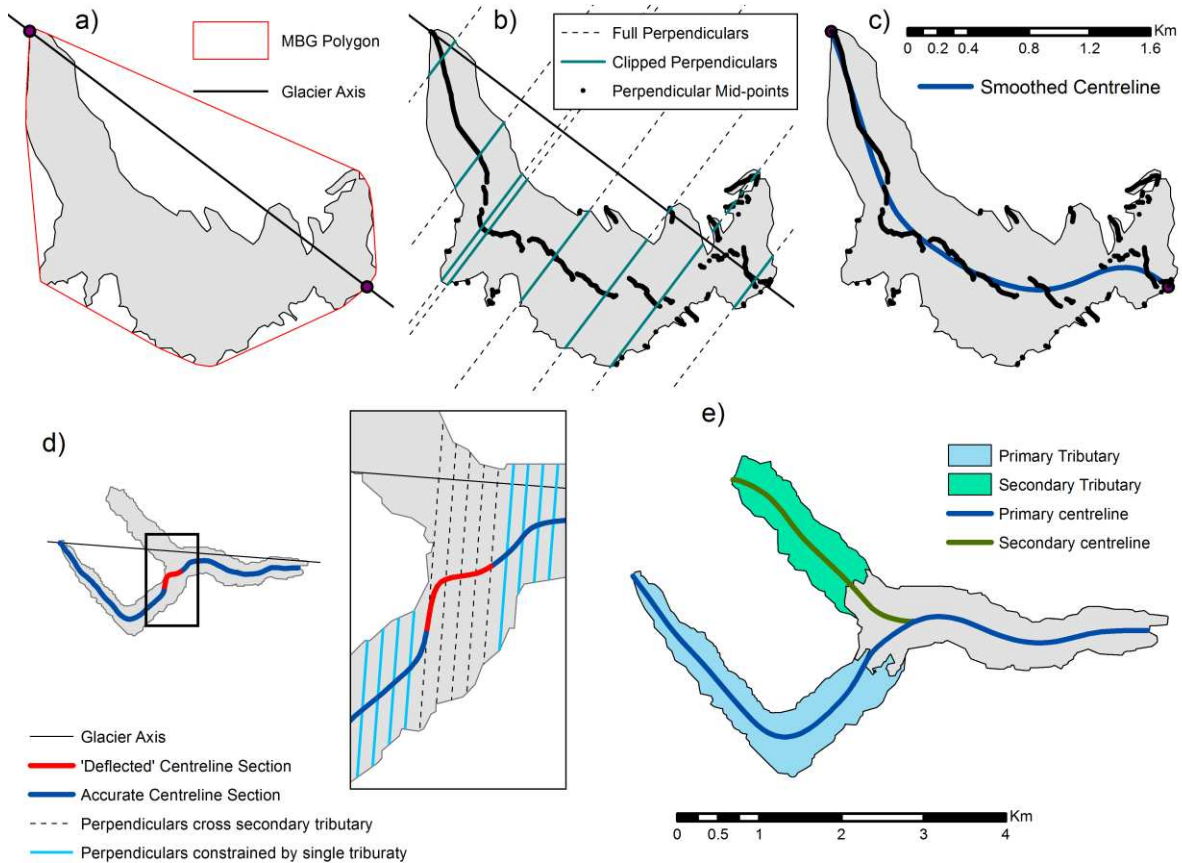
- 569 Linsbauer, A., F. Paul and W. Haeberli. 2012. Modeling glacier thickness distribution and bed
570 topography over entire mountain ranges with GlabTop: Application of a fast and robust
571 approach. *Journal of Geophysical Research*, **117**(F3).
- 572 Linsbauer, A. et al. 2009. The Swiss Alps without glaciers – a GIS-based modelling approach for
573 reconstruction of glacier beds. *In: Proceedings of Geomorphometry 2009, Zurich, Switzerland*.
- 574 Machguth, H. and M. Huss. 2014. The length of the glaciers in the world: a straightforward method
575 for the automated calculation of glacier center lines. *The Cryosphere Discussions*, **8**(3),
576 pp.2491-2528.
- 577 McNabb, R. et al. 2012. Using surface velocities to calculate ice thickness and bed topography: a case
578 study at Columbia Glacier, Alaska, USA. *Journal of Glaciology*, **58**(212), p1151.
- 579 Meier, M. F. et al. 2007. Glaciers dominate eustatic sea-level rise in the 21st century. *Science*,
580 **317**(5841), pp.1064-1067.
- 581 Michel, L. et al. 2013. Estimating the ice thickness of mountain glaciers with an inverse approach using
582 surface topography and mass-balance. *Inverse Problems*, **29**(3), p035002.
- 583 Nye, J. 1951. The flow of glaciers and ice-sheets as a problem in plasticity. *Proceedings of the Royal
584 Society of London. Series A. Mathematical and Physical Sciences*, **207**(1091), pp.554-572.
- 585 Nye, J. 1965. The flow of a glacier in a channel of rectangular, elliptic or parabolic cross-section. *Journal
586 of Glaciology*, **5**, pp.661-690.
- 587 Oerlemans, J. et al. 1998. Modelling the response of glaciers to climate warming. *Climate Dynamics*,
588 **14**(4), pp.267-274.
- 589 Paterson, W. S. B. 1994. *The physics of glaciers*. 3rd ed. Oxford: Pergamon.
- 590 Pellikka, P. and W. G. Rees. 2009. *Remote sensing of glaciers: techniques for topographic, spatial and
591 thematic mapping of glaciers*. CRC Press.
- 592 Radić, V. and R. Hock. 2010. Regional and global volumes of glaciers derived from statistical upscaling
593 of glacier inventory data. *Journal of Geophysical Research*, **115**(F1).
- 594 Schiefer, E., B. Menounos and R. Wheate. 2008. An inventory and morphometric analysis of British
595 Columbia glaciers, Canada. *Journal of Glaciology*, **54**(186), pp.551-560.
- 596 Schilling, D. and J. Hollin. 1981. Numerical reconstructions of valley glaciers and small ice caps. *In: P.
597 HUGHES and D. GH, eds. The Last Great Ice Sheets*. New York: John Wiley and Sons, pp.207-
598 221.
- 599 Schrott, L. et al. 2003. Spatial distribution of sediment storage types and quantification of valley fill
600 deposits in an alpine basin, Reintal, Bavarian Alps, Germany. *Geomorphology*, **55**(1), pp.45-63.
- 601 Shean, D. E., J. W. Head and D. R. Marchant. 2007. Shallow seismic surveys and ice thickness estimates
602 of the Mullins Valley debris-covered glacier, McMurdo Dry Valleys, Antarctica. *Antarctic
603 Science*, **19**(4), pp.485-496.
- 604 Singh, S. et al. 2012. Estimation of glacier ice thickness using Ground Penetrating Radar in the
605 Himalayan region. *Current Science (Bangalore)*, **103**(1), pp.68-73.
- 606 Span, N., A. Fischer and M. Kuhn. 2005. *Radarmessungen der Eisdicke österreichischer Gletscher [1995-
607 1998]: Messungen 1995 bis 1998*. Zentralanstalt für Meteorologie und Geodynamik.
- 608 Staines, K. E. and J. L. Carrivick. 2015. Geomorphological impact and morphodynamic effects on flow
609 conveyance of the 1999 jökulhlaup at Sólheimajökull, Iceland. *Earth Surface Processes and
610 Landforms*, **40**(10), pp.1401–1416.
- 611 USGS. 2014. *USGS, and Japan ASTER Program (2003)*. Sioux Falls.
- 612
- 613
- 614
- 615
- 616
- 617



618

619 **Fig. 1.** Flowchart conceptually illustrating the automatic generation of glacier centrelines and

620 estimation of distributed ice thickness and volume with VOLTA.

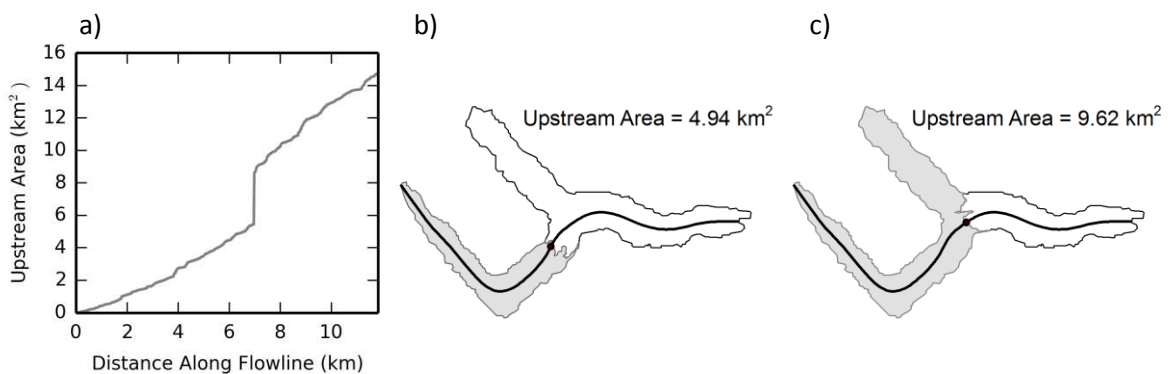


621

622

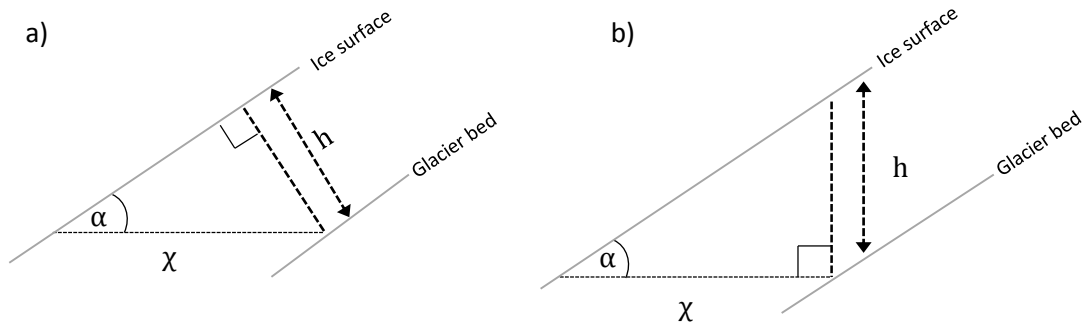
623 **Fig. 2.** VOLTA centreline production: a) definition of glacier axis via a polygon of minimum bounding
 624 geometry, b) creation of midpoints on perpendicular traverses, c) smoothed single centreline. Note
 625 that there can be unrealistic deflection of the centreline on multi-tributary glaciers (d), so VOLTA has
 626 developed a multi-centrelines model (e).

627



628

629 **Fig. 3.** a) Increase in upstream area as moving down centreline (for Unteraargletscher). Upstream area
 630 calculated before (b) and after (c) secondary branch.

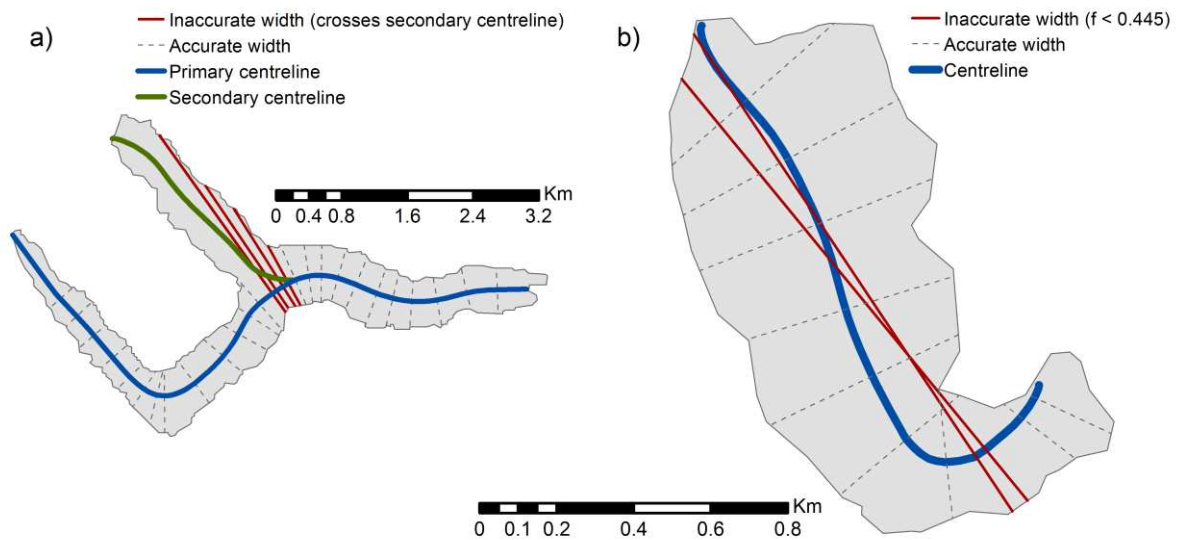


631

632 **Fig. 4.** a) Surface-perpendicular ice thickness calculated using the (original) sin function (Eq. 3) and b)
 633 vertical ice thickness calculated using the tan function (Eq. 4), as used by VOLTA.

634

635



636

637 **Fig. 5.** Inaccurate glacier width calculations identified where: (a) the perpendicular crosses an
 638 alternative centreline or (b) the resultant f value is < 0.445

639

640

641

642

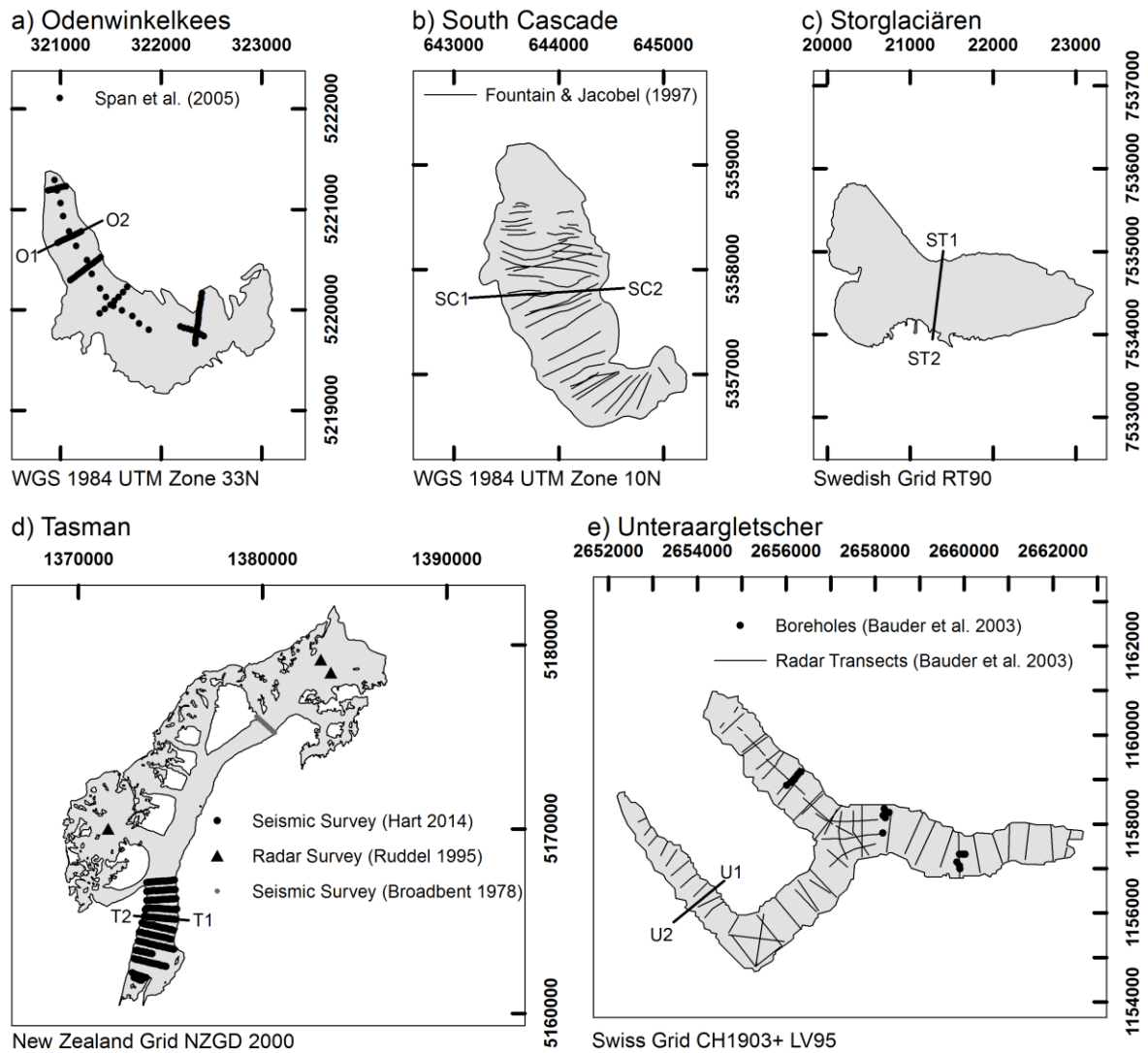
643

644

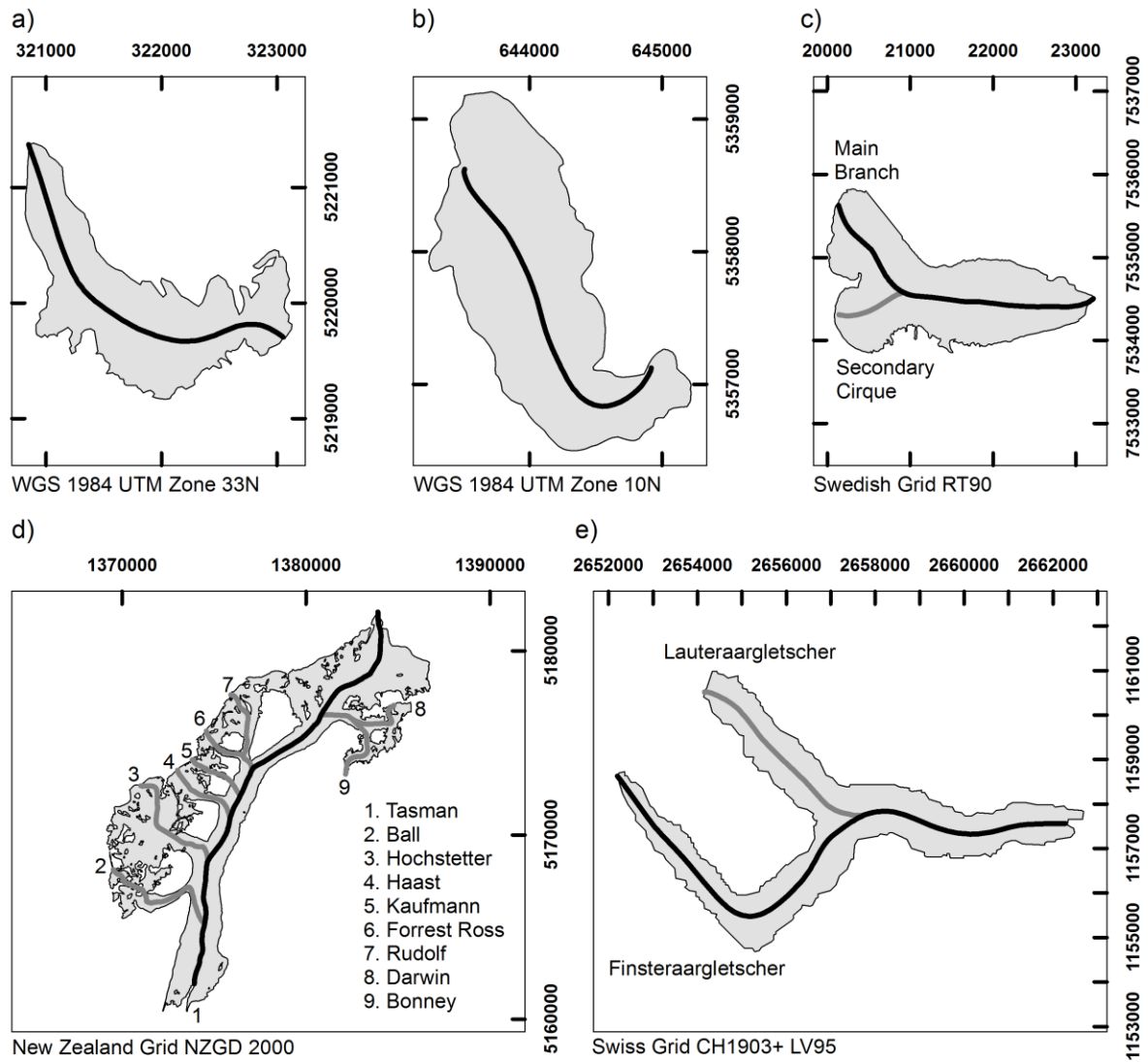
645

646

647



648 **Fig. 6.** Distribution of field measurements used to create bed topography datasets. Location of
649 transects used in Fig. 10 are also shown.



650 **Fig. 7.** Centrelines generated by VOLTA for sample glaciers. a) Ödenwinkelkees, b) South Cascade
651 glacier, c) Storglaciären, d) Tasman glacier, e) Unteraraargletscher

652

653

654

655

656

657

658

659

660

661

662

663
664
665
666
667
668
669
670
671
672
673
674
675
676
677
678
679
680
681

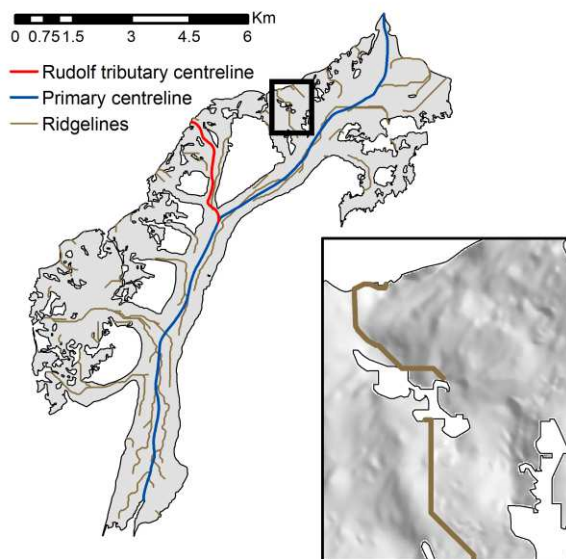
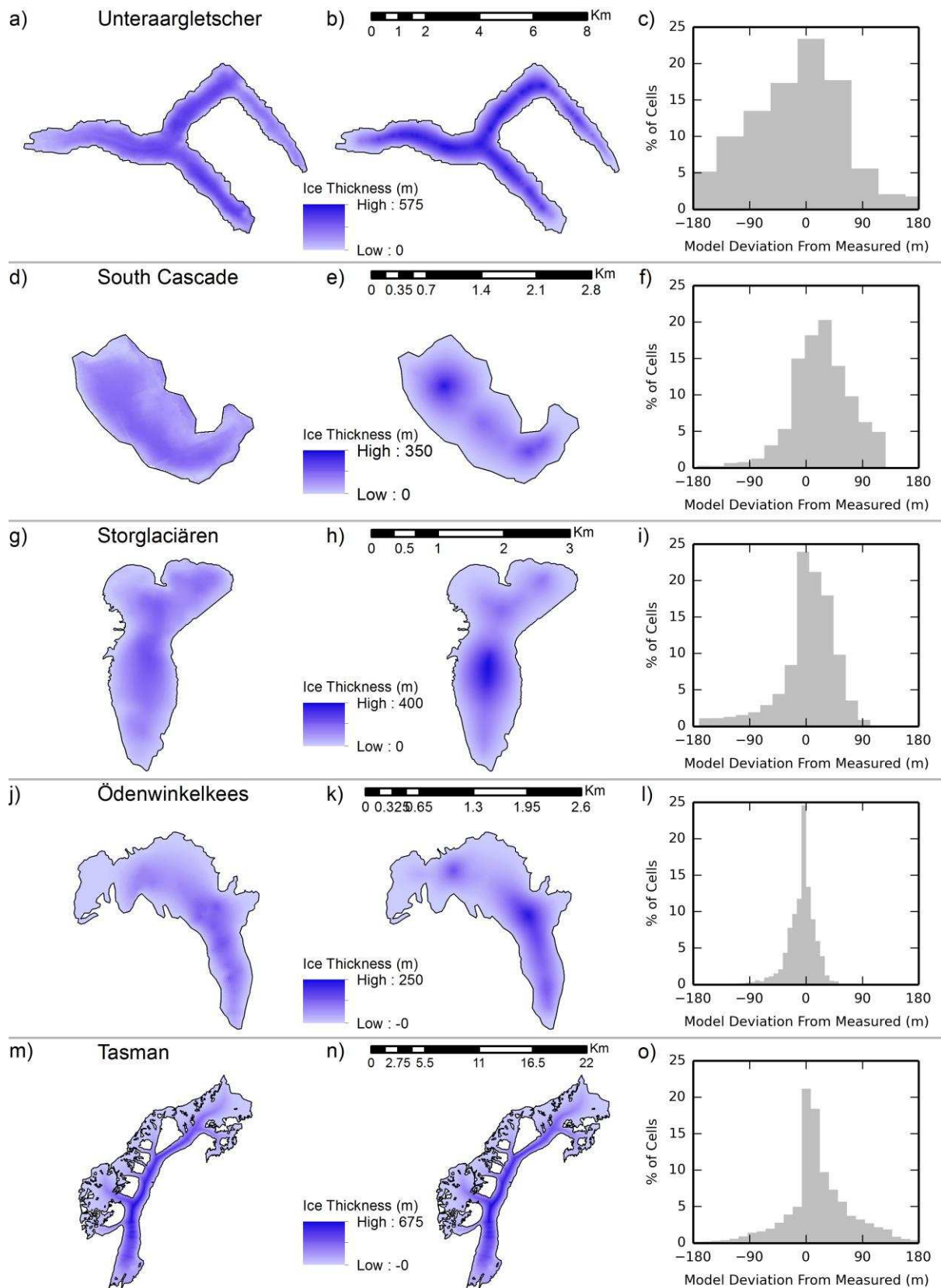


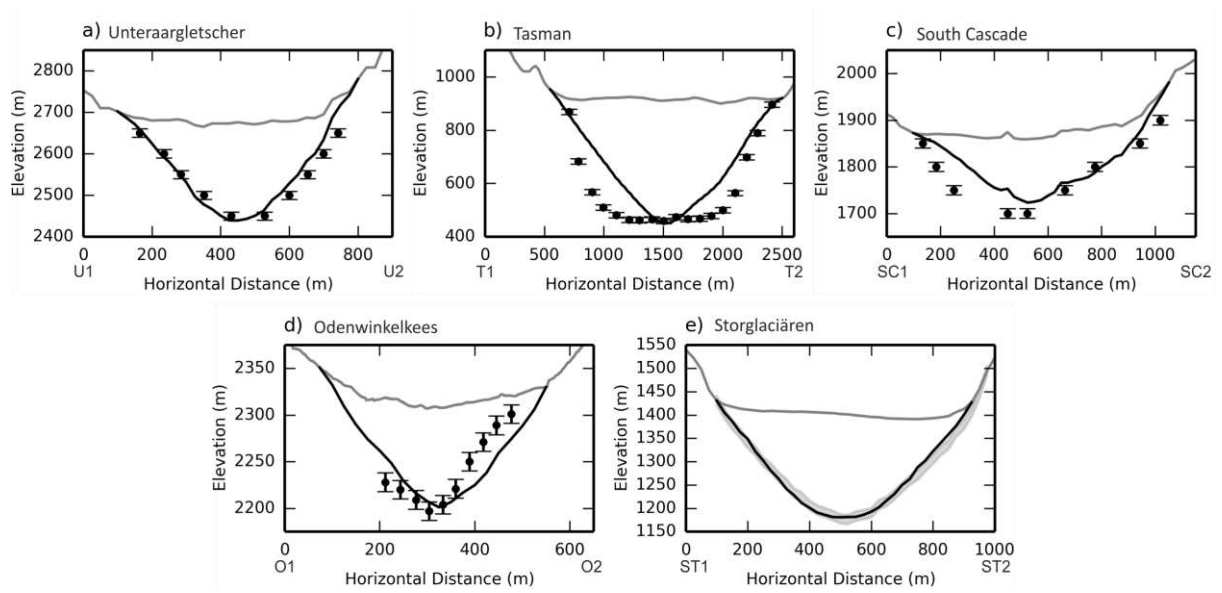
Fig. 8. GIS ridgeline network generated to indicated potential ice divide locations



682

683 **Fig. 9.** Field data derived (left) and VOLTA modelled (right) ice thickness maps with accompanying

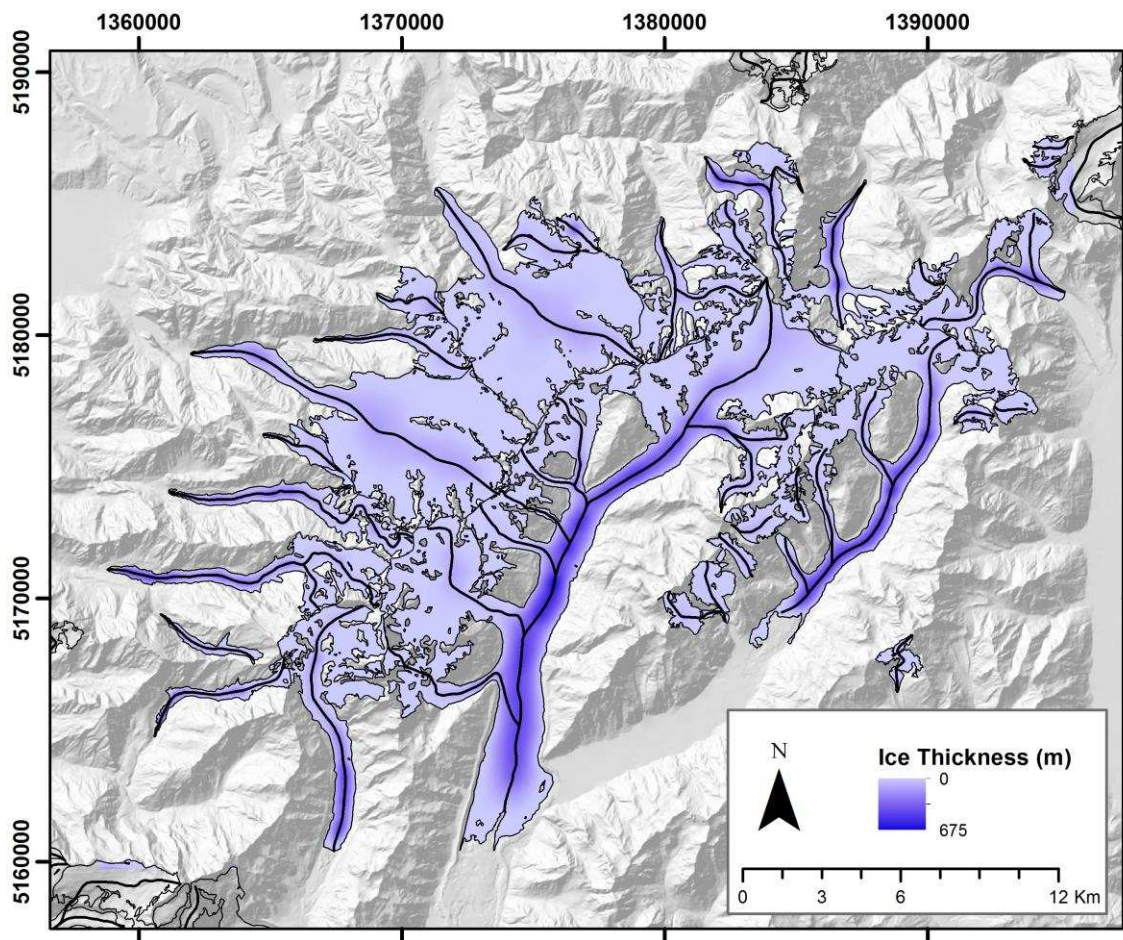
684 histograms showing the deviation of the modelled thickness from the measured.



685

686 **Fig. 10.** Comparison of traverse glacier-bed profiles generated by VOLTA (black lines) from field
 687 measurements (black dots). Panel e) shows field measurements as a grey band as it was provided as
 688 a pre-interpolated raster surface. For transect locations see Fig. 5.

689



690 **Fig. 11.** Automatically generated centrelines and ice thickness distribution for the Mt. Cook region

691

692

693

694

695

696

697

698

699

700

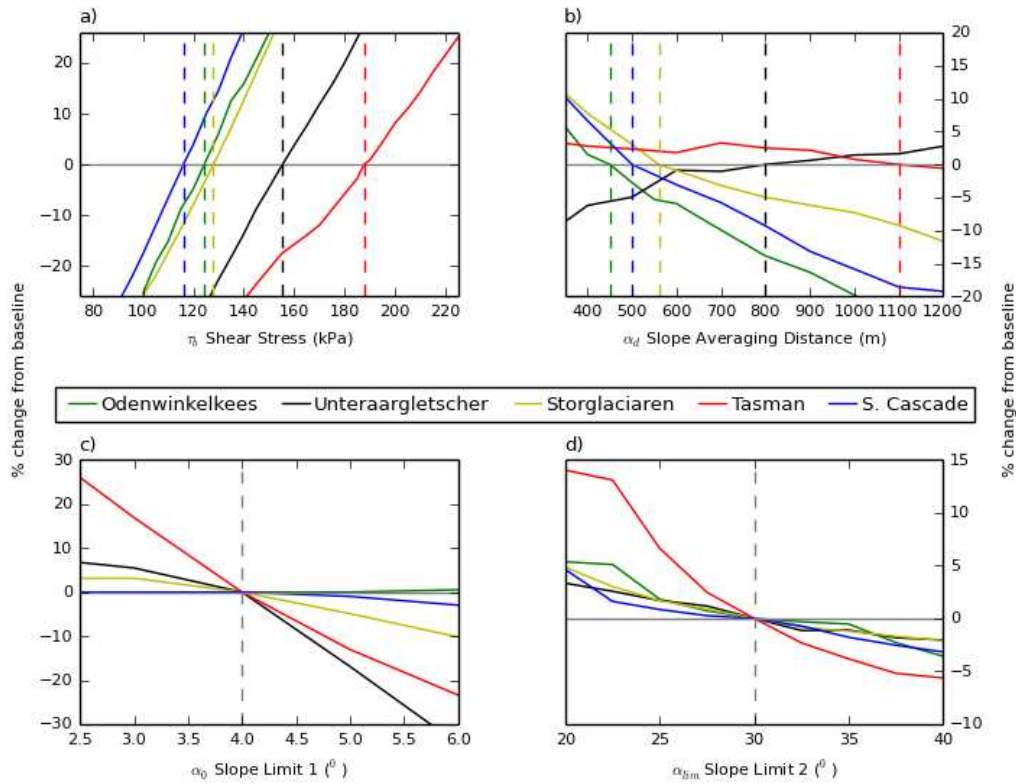
701

702

703

704

705



706
707
708
709
710

Fig. 12. Sensitivity of volume estimate to parameters: a) T_b , b) α_d , c) α_0 and d) α_{lim} . The solid grey horizontal lines represent a zero change in volume and the vertical dashed grey lines indicate the baseline value.

Glacier	Location	Area (km ²)	Surface DEM	Outline	Bed topography
South Cascade	48.360° -121.058°	1.73	ASTER, 30m (USGS 2014)	Fountain and Jacobel (1997)	Interpolated from 50m bed contours (derived from 5000+ measurements from multiple GPR transects) (Fountain and Jacobel 1997)
Ödenwinkelkees	47.111° 12.643°	1.9	LIDAR, 2m (Carrivick et al. 2013)	GLIMS (GLIMS 2014)	Interpolated from 77 GPR measurements (Span et al. 2005)
Storglaciären	67.902° 18.566°	3.2	10m, Composite dataset (e.g. Björnsson 1981)	Composite dataset (e.g. Björnsson 1981)	Composite dataset (e.g. Björnsson 1981)
Tasman	43.6166° 170.200°	90.4	Land Information New Zealand (LINZ), 15m	GLIMS (GLIMS 2014)	Interpolated from 14 transects (seismics) (Hart 2014) & (Broadbent 1974)
Unteraargletscher	46.566° 8.216°	14.6	ASTER, 30m (USGS 2014)	Bauder et al. (2003)	Interpolated from 50m bed contours (derived from radar transects and 27 boreholes) (Bauder et al. 2003)

711
712
713
714
715

Table 1. Location of each glacier and details of the datasets used for determining the ‘field derived’ volume and VOLTA inputs.

Glacier	Volume (field measurements), km ³	Volume VOLTA, km ³	Volume Difference, %	Estimated shear stress, kPa	Slope averaging window, m	Median deviation, m	Deviation IQR, m
South Cascade	0.200	0.147	-26.5	115	500	25.8	59.0
Ödenwinkelkees	0.078	0.091	16.6	124	450	-2.7	22.3
Storglaciären	0.292	0.282	-3.4	127	550	7.7	42.4
Tasman	12.040	10.062	-16.4	187	1000	13.6	46.7
Unteraargletscher	2.983	3.279	9.9	155	800	-11.2	112.6

716

717

718 **Table 2.** Comparison between volumes calculated from field based observations and modelled by
719 VOLTA. Parameters derived and summary statistics are also shown. Deviation is defined as the
720 modelled (VOLTA) ice thickness subtracted from field measured value for each cell.